Original Article

The role of chromatin modulator DPY30 in glucose metabolism of colorectal cancer cells

Xiaomei Mao[1,2#^], Shiqin Yang[1#], Ye Zhang[1], Huajun Yang[1], Danhong Yan[1], Lingzhi Zhang[1]

[1]Department of Medical Science and Technology, Suzhou Chien-Shiung Institute of Technology, Taicang, China; [2]School of Life Sciences, Xiamen University, Xiamen, China

Contributions: (I) Conception and design: X Mao; (II) Administrative support: S Yang; (III) Provision of study materials or patients: Y Zhang; (IV) Collection and assembly of data: X Mao, S Yang; (V) Data analysis and interpretation: H Yang, D Yan, L Zhang; (VI) Manuscript writing: All authors; (VII) Final approval of manuscript: All authors.

[#]These authors contributed equally to this work.

Correspondence to: Xiaomei Mao, MD. Department of Medical Science and Technology, Suzhou Chien-Shiung Institute of Technology, 1 Jianxiong Road, Taicang 215411, China; School of Life Sciences, Xiamen University, Xiamen, China. Email: 9206@csit.edu.cn.

Background: Colorectal cancer (CRC) is the third most common cancer worldwide and the second leading cause of cancer-related death. This study investigated the role of DPY30 in the development and progression of CRC cells, especially in the area of cellular glycolysis.

Methods: HT29 control cells and DPY30 knockdown cells were collected for tandem mass tag (TMT) labeling quantitative proteomics analysis of cellular total proteins (n=3). To further assess the accuracy of the differential expression profile, representative genes were selected and confirmed by quantitative real-time polymerase chain reaction (qPCR) and western blot (WB). Glycolytic flux was studied by detecting the extracellular acidification rate (ECAR) using the Seahorse XFe96. In view of the vital role of DPY30 on the H3K4me3 level, chromatin immunoprecipitation (ChIP) assays were performed.

Results: The results showed that the expression of HK1, a protein related to cellular glucose metabolism, was significantly down-regulated after DPY30 knockdown, while the expression of GSK3B was significantly increased. Kyoto Encyclopedia of Genes and Genomes (KEGG) pathway analysis indicated significant changes in several signaling pathways, with the PI3K-AKT signaling pathway being the most prominent. The data of Seahorse XFe96 revealed that DPY30 knockdown attenuated aerobic glycolysis. DPY30 knockdown repressed the establishment of H3K4me3 on promoters of *HK1*, *PFKL*, and *ALDOA*.

Conclusions: DPY30 promoted the glycolysis of CRC cells through two channels: influencing signaling pathways and gene transcription, thereby promoting the progression of CRC.

Keywords: DPY30; glycolysis; colorectal cancer (CRC); PI3K-AKT signaling pathway

Submitted Mar 07, 2024. Accepted for publication Jun 30, 2024. Published online Aug 16, 2024.
doi: 10.21037/tcr-24-366
View this article at: https://dx.doi.org/10.21037/tcr-24-366

Introduction

According to statistics from the GLOBOCAN project of the International Agency for Research on Cancer (IARC), in 2020, colorectal cancer (CRC) was the third most common cancer worldwide and the second leading cause of cancer-related death (1). There are significant regional differences in the burden of CRC, with the highest incidence and mortality typically observed in countries with a high human development index (HDI), such as Europe, Oceania, and

^ ORCID: 0009-0009-1067-650X.

North America (2). In recent years, with the development of social economy, the "westernization" of lifestyle and dietary habits, the incidence and mortality of CRC have increased significantly in China (3). Most patients are diagnosed at an advanced stage. Cancer screening could help reduce the incidence and mortality of CRC.

The progression of CRC is a complex and dynamic process, characterized by typical features of malignant cells, including unlimited replicative potential, resistance to apoptotic signals, tissue invasion, and metastasis. To acquire and sustain the energy and materials required for these characteristics, malignant cells must reprogram their own metabolic pathways. The metabolic process of cancer cells differs from that of normal tissue cells, with glycolysis and glucose metabolism being the most significantly altered metabolic pathways. The Warburg effect suggests that tumor cells prefer highly active glycolysis to meet their survival needs (4). The reprogramming of these pathways involves intricate mechanisms and the coordination of various signaling molecules. Understanding the mechanisms of glycolysis in the progression of CRC provides a new perspective for the discovery of screening targets and treatment approaches.

Epigenetics, especially histone modifications, is an important factor in altering gene expression in CRC cells (5). In mammals, the SET1/MLL complex (COMPASS family) is one of the major H3K4 methyltransferases (KMTs). The SET1/MLL complex is a potential drug target in epigenetic therapy because of their extensive association with various cancers (6,7). SET1/MLL complexes are comprised of one of the six different catalytic subunits (SETD1A, SETD1B, MLL1, MLL2, MLL3, and MLL4) and conserved core subunits. WDR5, RBBP5, ASH2L, and DPY30 (together as WRAD) are called core subunits (8-10). The catalytic subunits have intrinsic methyltransferase activity, which is weak in the absence of core subunits. Core subunits, including DPY30, lack or have very weak intrinsic catalytic activity, but they are essential for biologically significant H3K4 methylation levels in cells (11-13).

DPY30 was first identified as a dose compensation-related gene in C. elegans (14), and it was important for the behavior of the worm. Previous studies on DPY30 had focused on the stem cell function, cell senescence, adhesion, migration, and invasion (15-17). Gradually, its role in the development of tumors has been explored. Reports demonstrated that DPY30 was related to the proliferation, migration, and invasion of gastric cancer, cholangiocarcinoma, and hepatocellular carcinoma cells (18-20). In this study, we investigated the role of DPY30 in the development and progression of CRC, especially on cellular glycolysis. We present this article in accordance with the ARRIVE and MDAR reporting checklists (available at https://tcr.amegroups.com/article/view/10.21037/tcr-24-366/rc).

Highlight box

Key findings

- DPY30 promoted the glycolysis of colorectal cancer (CRC) cells through two channels: influencing signaling pathways and gene transcription, thereby promoting the progression of CRC.

What is known and what is new?

- DPY30 was overexpressed in CRC tissues. DPY30 promoted the proliferation and cell cycle progression of CRC cells.
- DPY30 knockdown attenuated aerobic glycolysis. DPY30 knockdown repressed the establishment of H3K4me3 on promoters of *HK1*, *PFKL*, and *ALDOA*. The changes of glycolysis were also related to PI3K-AKT signaling pathway.

What is the implication, and what should change now?

- Our study provides a theoretical basis for a comprehensive explanation of the role of DPY30 in CRC formation, especially on the study of glycolysis. This study reveals DPY30 as a potential cancer therapeutic target.

Methods

Cell culture

The CRC cells KM12C and HT29 were obtained from Procell (Wuhan, China), cultured in Dulbecco's modified Eagle medium (DMEM) complete medium, which contained 10% fetal bovine serum, 100 U/mL penicillin, and 100 μg/mL streptomycin. The cells were cultured in an environment at 37 ℃ with 5% CO_2 and adequate humidity. The lentiviral knockdown of DPY30 in KM12C and HT29 cells was established in our previous study using short hairpin RNA (shRNA) (21). The established cells were also cultured using the aforementioned standard methods.

Animals

Male nude mice (BALB/c, 6 weeks old, 18–20 g) were obtained from the Xiamen University Laboratory Animal Center. HT29 cells were used to build the model according to our previous study (21). Mice were housed in a suitable environment free of specific pathogens, and randomly divided into two groups—shCtrl and shDPY30 (n=6 in

each group, 12/12 cycle of light, 25–27 ℃). Changes in tumor weight and protein levels were measured. Animal experiments were performed according to ethical guidelines of animal experiment and reviewed and approved by the Institutional Animal Care and Use Ethics Committee of Xiamen University (No. XMULAC20180077), in compliance with national guidelines for the care and use of animals. A protocol was prepared before the study without registration.

Antibodies

Anti-DPY30 (cat. #ab126352), anti-HK1 (cat. #ab154839), and anti-GSK3 beta (cat. #ab93926) antibodies were purchased from Abcam (Cambridge, UK). Anti-Akt (pan) (cat. #2920), anti-phospho-Akt (Thr308) (cat. #13038), and anti-phospho-Akt (Ser473) (cat. #4060) antibodies were from Cell Signaling Technology (CST; Danvers, MA, USA). Anti-Beta Tubulin antibody was from Proteintech (Wuhan, China).

Quantitative real-time polymerase chain reaction (qPCR)

The extraction and reverse transcription of cellular RNA were performed using a total RNA extraction kit (cat. #DP419) and a reverse transcription kit (cat. #KR116; TIANGEN, Beijing, China), following the instructions. The complementary DNA (cDNA) obtained by reverse transcription was diluted tenfold with DNase/RNase-free deionized water as a template. The primers were diluted to a 100 μM stock solution with deionized water and further diluted tenfold before use. Next, a reaction mixture was prepared using the TIANGEN's SuperReal PreMix Plus (SYBR Green) (cat. #FP205) reagent kit. The reaction system was composed of 5 μL enzyme mixture, 0.3 μL each of 10 μM forward and reverse primers, 1 μL of the diluted cDNA template, 0.2 μL ROX instrument calibration solution, and 3.2 μL RNase-free ddH_2O. The fluorescence quantitative PCR instrument (ABI 7500) used for this procedure required ROX calibration. Based on the characteristics of enzymes in the kit, the qPCR reaction procedure was set up, and reaction conditions were optimized according to different primers.

Western blot (WB)

First, the total cellular protein was extracted. The adherent cells were gently rinsed three times with pre-cooled phosphate-buffered saline (PBS). On the final rinse, radioimmunoprecipitation assay (RIPA) lysis buffer containing protease/phosphatase inhibitors was added to the culture dish. After being lysed on ice, the cells were scraped into a centrifuge tube. Then cells in the tube were vortexed and centrifuged. The proteins obtained from the lysed cells were frozen in the refrigerator at –80 ℃ or measured immediately. Standard curves were prepared and samples were measured by Pierce Bicinchoninic Acid (BCA) Protein Assay Kit (cat. #23225; ThermoFisher Scientific, Wilmington, DE, USA).

WB samples were prepared according to the measured protein concentrations. Protein bands were separated by electrophoresis and then transferred to the polyvinylidene fluoride (PVDF) membrane. The membrane was blocked using skim milk or bovine serum albumin (BSA) at room temperature for 1 h and incubated with the primary antibody and the secondary antibody. Protein bands were visualized using the electrochemiluminescence (ECL) reagent (cat. #32106; ThermoFisher Scientific). The WB experiment was repeated at least three times. Among them, the representative WB graph is selected to be displayed in figures.

Tandem mass tag (TMT) labeling quantitative proteomics analysis of cellular total proteins

Control cells and cells with DPY30 knockdown were seeded into 9 cm dishes and grown to approximately 80% confluence. Next, the cells were washed with pre-cooled PBS, and collected into the centrifuge tube with cell scraper. The supernatant was removed by the centrifuge. Then the tubes were sent on dry ice to Xiamen Lifeint Technology Co., Ltd. (Xiamen, China) to complete the following steps: quality control of protein extraction, enzymatic digestion, TMT labeling, liquid chromatography-mass spectrometry analysis, and data analysis.

Oxygen consumption rate (OCR) and extracellular acidification rate (ECAR)

The Seahorse XF extracellular flux analyzer (Agilent, Santa Clara, CA, USA) was used to assess the OCR and ECAR of cells according to instructions. Briefly, cells were seeded in microplates overnight to make them adhere to the wall. Next day, cells were washed and growth medium was replaced with assay medium. Then, stock compounds of each assay were prepared and injected into corresponding

Table 1 Primers and oligos

Gene	Application	Species	Forward primer (5'-3')	Backward primer (5'-3')
DPY30	Expression	Human	AACGCAGGTTGCAGAAAATCCT	TCTGATCCAGGTAGGCACGAG
GSK3B	Expression	Human	GGCAGCATGAAAGTTAGCAGA	GGCGACCAGTTCTCCTGAATC
HK1	Expression	Human	GCTCTCCGATGAAACTCTCATAG	GGACCTTACGAATGTTGGCAA
HK2	Expression	Human	GAGCCACCACTCACCCTACT	CCAGGCATTCGGCAATGTG
PFKL	Expression	Human	GCTGGGCGGCACTATCATT	TCAGGTGCGAGTAGGTCCG
ALDOA	Expression	Human	ATGCCCTACCAATATCCAGCA	GCTCCCAGTGGACTCATCTG
PC	Expression	Human	ACAGAGGTGAGATTGCCATCC	CACTGCATCTACGTTGTTCTCC
Glut1	Expression	Human	GGCCAAGAGTGTGCTAAAGAA	ACAGCGTTGATGCCAGACAG
G6PD	Expression	Human	CGAGGCCGTCACCAAGAAC	GTAGTGGTCGATGCGGTAGA
α-tublin	Expression	Human	CCAAGCTGGAGTTCTCTA	CAATCAGAGTGCTCCAGG
β-actin	Expression	Human	CATGTACGTTGCTATCCAGGC	CTCCTTAATGTCACGCACGAT
Scramble	shCtrl	Human	CCGGGGCTACGTCCAGGAGCGCACCCTCGAGGGTGCGCTCCTGGACGTAGCCTTTTTG	AATTCAAAAAGGCTACGTCCAGGAGCGCACCCTCGAGGGTGCGCTCCTGGACGTAGCC
DPY30	shDPY30-1	Human	CCGGGACCACCAAATCCCATTGAATCTCGAGATTCAATGGGATTTGGTGGTCTTTTTG	AATTCAAAAAGACCACCAAATCCCATTGAATCTCGAGATTCAATGGGATTTGGTGGTC
DPY30	shDPY30-2	Human	CCGGCACAGTTTGAAGATCGAAACCTCGAGGTTTCGATCTTCAAACTGTGTTTTTG	AATTCAAAAACACAGTTTGAAGATCGAAACCTCGAGGTTTCGATCTTCAAACTGTG
GSK3B	ChIP	Human	AGCGCTTTATAGACGCCCTC	CCAGAGACGCTGGTGAAACT
HK1	ChIP	Human	GTCATCCCTCCCTCTGATTTG	CCTCAGTCTTGCTGGACTTTAT
PFKL	ChIP	Human	CTCAAATCCTAGCGATCAGC	AAAGCAGCCAGCACTCCTCC
ALDOA	ChIP	Human	CTGTGGAAATGTGAGACCCTAC	CCTCCCAAAGTGCTAGGATTAC

sh, short hairpin; ChIP, chromatin immunoprecipitation.

ports. The Seahorse XF Report Generator was used to analyze the data.

Chromatin immunoprecipitation (ChIP) assay

SimpleChIP® Plus Sonication ChIP Kit (cat. #56383) from CST (using a 10 cm culture dish as an example) was used in this experiment. Primers and oligos used for qPCR, shRNA and ChIP assays are attached in *Table 1*.

Cell preparation

Cells were seeded and treated, and the final volume of the culture medium was 10 mL.

Sample cross-linking

Two hundred and seventy μL of 37% formaldehyde was added to each dish and cross-linked for 15 minutes after mixing. Add 1 mL of 10× glycine to each dish and incubate for 5 minutes to terminate the cross-linking. Place the dishes on ice. Remove the culture medium, rinse the cells twice with pre-cooled PBS, and gently scrape the cells into 1 mL of PBS. Centrifuge at 4 ℃ for 5 minutes at 1,000 g to remove the supernatant.

Chromatin fragmentation (performed on ice)

Up to 2×10^7 cells were re-suspended and lysed in 1 mL lysis buffer (containing protease inhibitors). Next, centrifuge at 5,000 g for 5 minutes, remove the supernatant, and replace the lysis buffer with ChIP sonication nuclear lysis buffer. Lyse the cells for 10 minutes and then sonicate to break the chromatin. The sonication parameters needed optimization for different cell types. After centrifuging at 21,000 g for 10 minutes, collect the supernatant, and store the fragmented chromatin at –80 ℃.

Analysis the efficiency of chromatin fragmentation

Take a 50 µL of the supernatant for analysis. Perform agarose gel electrophoresis to assess the size and concentration of the fragmented chromatin.

ChIP

Approximately 4×10^6 cells were required for each precipitation reaction. Before adding antibodies, the chromatin was diluted with the buffer. Before adding antibodies, dilute the chromatin with the buffer at a 1:4 ratio. A 10 µL diluted chromatin sample was taken as a 2% input control and stored at –20 ℃. Next, samples were incubated with antibodies or normal rabbit immunoglobulin G (IgG) (negative control) at 4 ℃ with rotation overnight. A 30 µL of protein G magnetic beads was added for each immunoprecipitation reaction and incubated at 4 ℃ with rotation for 2 h. Magnetic beads were washed three times with the low salt solution and one time with the high salt solution using a magnetic rack.

Chromatin elution

Add a 150 µL of elution buffer to each ChIP sample. Elute at 65 ℃ for 30 minutes. Gently shake the samples every 5 minutes. Centrifuge the samples at 10,000 g for 10 s to concentrate them at the bottom of the centrifuge tube. Carefully aspirate the supernatant using a magnetic rack. All samples (including 2% input) were added with 6 µL 5 M NaCl and 2 µL protease K, and incubated at 65 ℃ for 2 h or overnight. The resulting sample could be stored for up to 4 days at –20 ℃ or immediately purified for the next step.

Analysis and calculation

Measure the concentration of DNA and perform qPCR analysis. Calculate the enrichment efficiency of ChIP-qPCR: % input = $2\% \times 2^{[\text{cycle threshold (CT) input} - \text{CT sample}]}$.

Statistical analysis

Data processing and analysis were performed using GraphPad Prism 8, EXCEL, and IBM SPSS Statistics 22. All data were collected with three or more replicates, and statistics were presented as mean ± standard error of mean (SEM). The independent samples *t*-test (for normally distributed data) or the Mann-Whitney *U* test (for non-normally distributed data) was employed to compare any two groups. P<0.05 was marked as *; P<0.01 was marked as **; and P<0.001 was marked as ***.

Results

DPY30 was associated with proteins related to glucose metabolism

Our previous research found that DPY30 was overexpressed in CRC tissues. DPY30 promoted the transcription of *PCNA*, *Ki67*, and *cyclin A2* by mediating H3K4me3, thereby promoting the proliferation and cell cycle progression of CRC cells. This suggested that DPY30 served as a potential therapeutic molecular target for CRC (21). In this study, previously established cell models were used. First, the knockdown efficiency of DPY30 in cells was tested. At both the protein and messenger RNA (mRNA) levels, the shDPY30-2 segment showed better effectiveness in DPY30 knockdown, especially in HT29 cells (*Figure 1A*,*1B*). In the following studies, only cell lines constructed with the shDPY30-2 knockdown segment were used, abbreviated as shDPY30. Then, HT29 control cells and DPY30 knockdown cells were collected for TMT labeling quantitative proteomics analysis of cellular total proteins (n=3). After the threshold was defined, the down-knocked cells were compared with the control cells (shDPY30/shCtrl), and it was found that the expression of 256 proteins was up-regulated and that of 198 proteins was down-regulated. The differentially expressed genes of the control group and the shDPY30 group were further analyzed using a volcano plot (*Figure 1C*). The results showed that the expression of HK1, a protein related to cellular glucose metabolism, was significantly down-regulated after DPY30 knockdown, while the expression of GSK3B was significantly increased. Based on the differential gene expression, Kyoto Encyclopedia of Genes and Genomes (KEGG) pathway analysis, as shown in *Figure 1D*, indicated significant changes in several signaling pathways, with the PI3K-AKT signaling pathway being the most prominent. These results suggested that DPY30 played a role in the glucose metabolism of CRC cells.

DPY30 regulated genes related to glucose metabolism and the PI3K-AKT signaling pathway

To further assess the accuracy of the differential expression profile, representative genes were selected and confirmed by qPCR (*Figure 2A*). In addition to *GSK3B* and *HK1*, other genes associated with glucose metabolism were also examined. Consistent with the results of proteomic analysis, the expression of *GSK3B* was upregulated, while

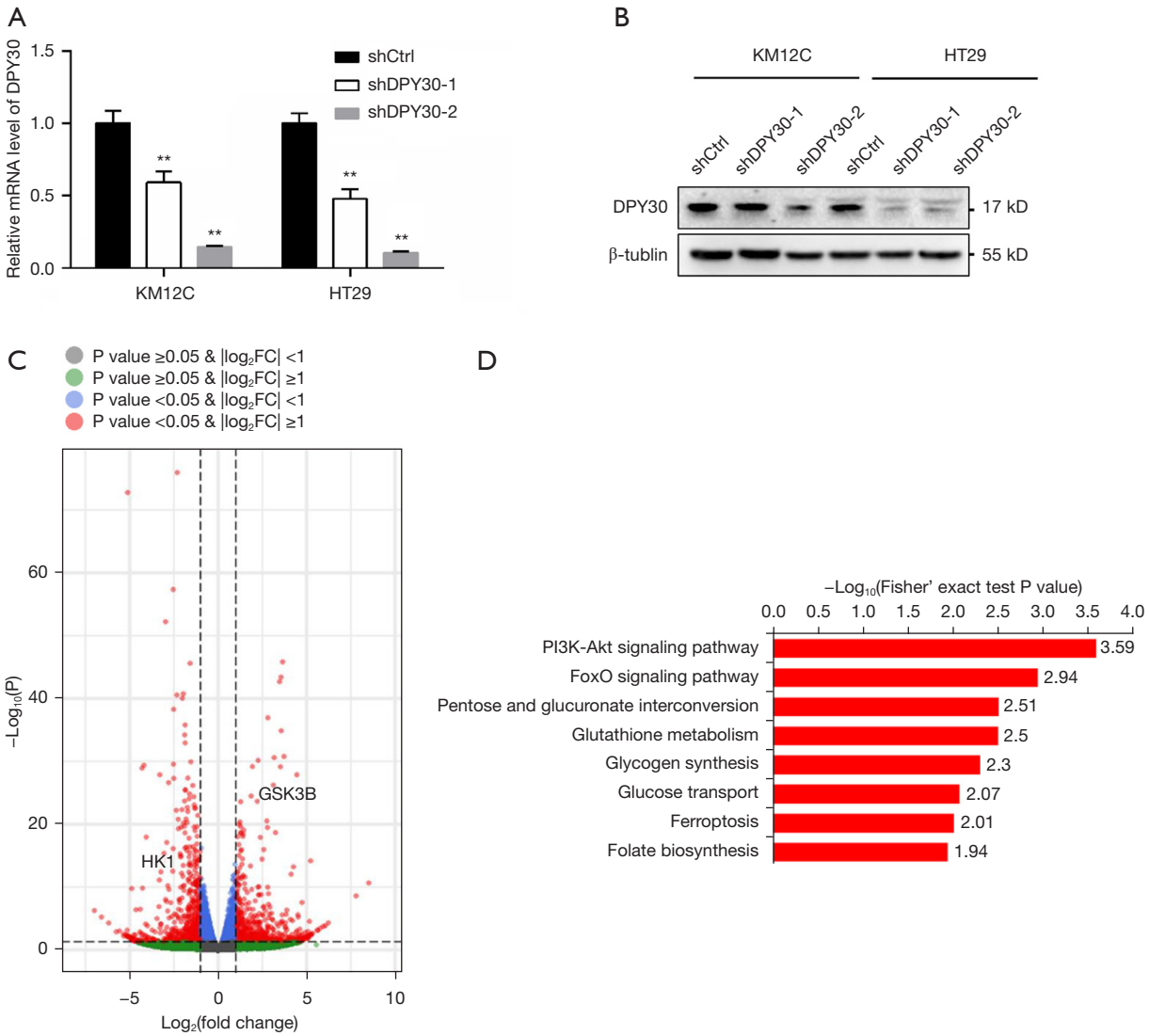

Figure 1 TMT labeling quantitative proteomics analysis of cellular total proteins (shDPY30 *vs.* shCtrl). (A,B) The knockdown efficiency of DPY30 in cells was tested using qPCR and WB. (C) The differentially expressed genes of the control group and the shDPY30 group were further analyzed using a volcano plot. (D) KEGG pathway analysis based on the differential gene expression. Data were expressed as mean ± SEM. n=3. **, P<0.01. mRNA, messenger RNA; sh, short hairpin; FC, fold change; TMT, tandem mass tag; qPCR, quantitative real-time polymerase chain reaction; WB, western blot; KEGG, Kyoto Encyclopedia of Genes and Genomes; SEM, standard error of mean.

that of *HK1* was downregulated. In addition, the expression of *PFKL* and *ALDOA* decreased in both cells. WB results showed that after DPY30 knockdown, the protein levels of HK1 also decreased, but the expression of GSK-3β increased only in the HT29 cell model. AKT is a serine/threonine-specific protein kinase that plays a crucial role in various cellular processes, such as glucose metabolism, apoptosis, cell proliferation, transcription, and cell migration. As shown in *Figure 2B*, p-AKT (Thr308) was found to decrease with a reduction in DPY30 expression. The expression of pan-AKT and p-AKT (Ser473) did not show significant changes. These findings confirmed the role of DPY30 in glucose metabolism and the PI3K-AKT signaling pathway.

DPY30 knockdown attenuated aerobic glycolysis

Aerobic glycolysis of tumor cells is one of the important characteristics of the tumor. Whether DPY30 influences the

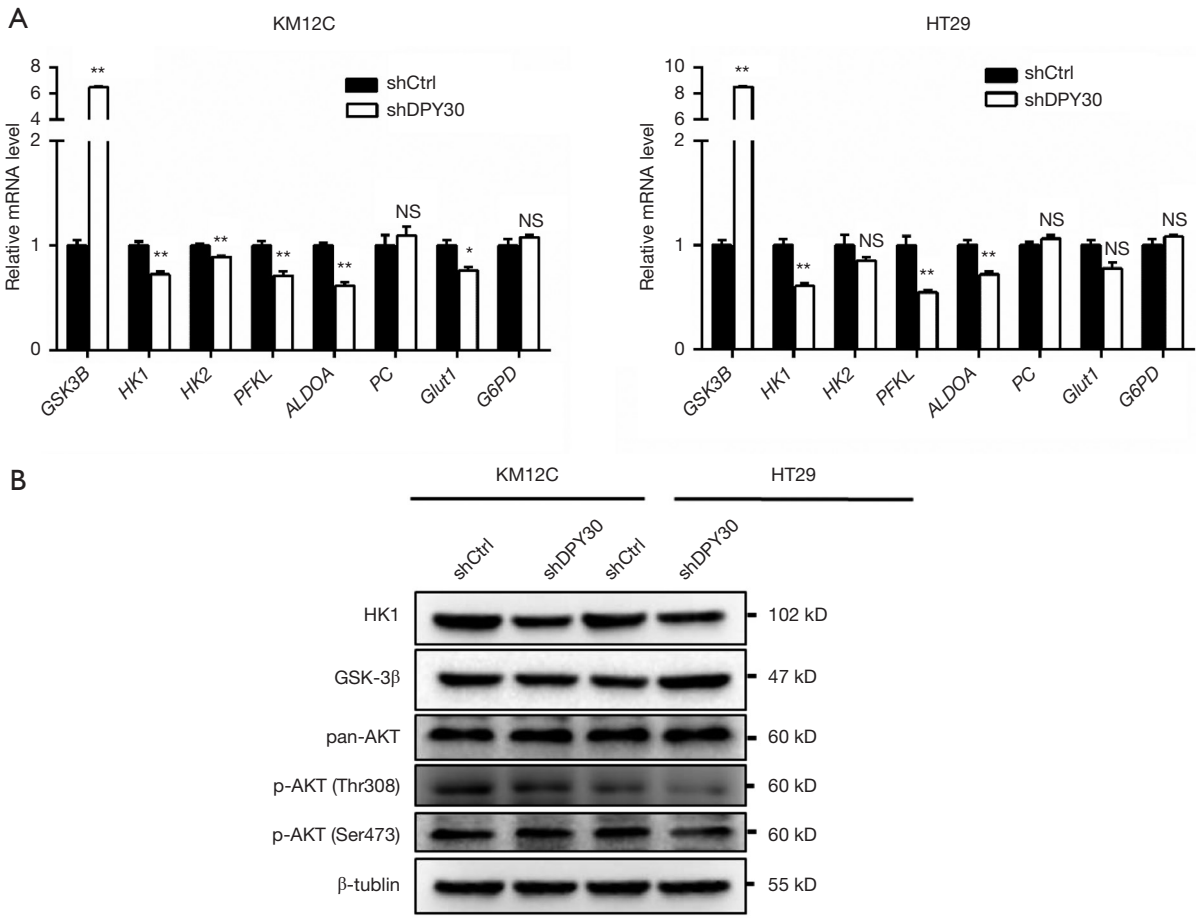

Figure 2 DPY30 regulated genes related to glucose metabolism and the PI3K-AKT signaling pathway. (A) Representative genes were selected and confirmed by qPCR in KM12C and HT29 cells. (B) Representative proteins were selected and confirmed by WB in KM12C and HT29 cells. Data were expressed as mean ± SEM. n=3. *, P<0.05; **, P<0.01. mRNA, messenger RNA; sh, short hairpin; NS, no significant difference; qPCR, quantitative real-time polymerase chain reaction; WB, western blot; SEM, standard error of mean.

glycolysis metabolic process of CRC cells is unknown. To address this issue, glycolytic flux was studied by detecting the ECAR using the Seahorse XFe96. As shown in *Figure 3A*,*3B*, the analysis data revealed that the knockdown of DPY30 reduced the overall glycolytic flux in HT29 and KM12C cells. Glycolysis, glycolytic capacity, and glycolytic reserve were remarkably decreased in DPY30 knockdown cells. Furthermore, oxidative phosphorylation was then investigated. Our data indicated that the levels of OCR were increased by the knockdown of DPY30 (*Figure 3C*,*3D*). Spare respiratory capacity was significantly increased in both cells. To sum up, the data indicated that the aerobic glycolysis of CRC cells was impaired by DPY30 knockdown.

DPY30 knockdown suppressed the establishment of H3K4me3 to target genes

DPY30 is a member of the mammalian SET1/MLL histone methyltransferase complex. Previous reports have demonstrated the role of DPY30 in regulating all three levels of H3K4 methylation, especially H3K4me3 (15). H3K4me3 localized at the promoter regions of actively transcribed genes (22). Obvious reductions in global H3K4me3 upon the knockdown of DPY30 were found.

In view of the vital role of DPY30 on the H3K4me3 level, ChIP assays were performed. The qPCR data revealed that DPY30 knockdown repressed the establishment of H3K4me3 on promoters of *HK1*, *PFKL*, and *ALDOA*

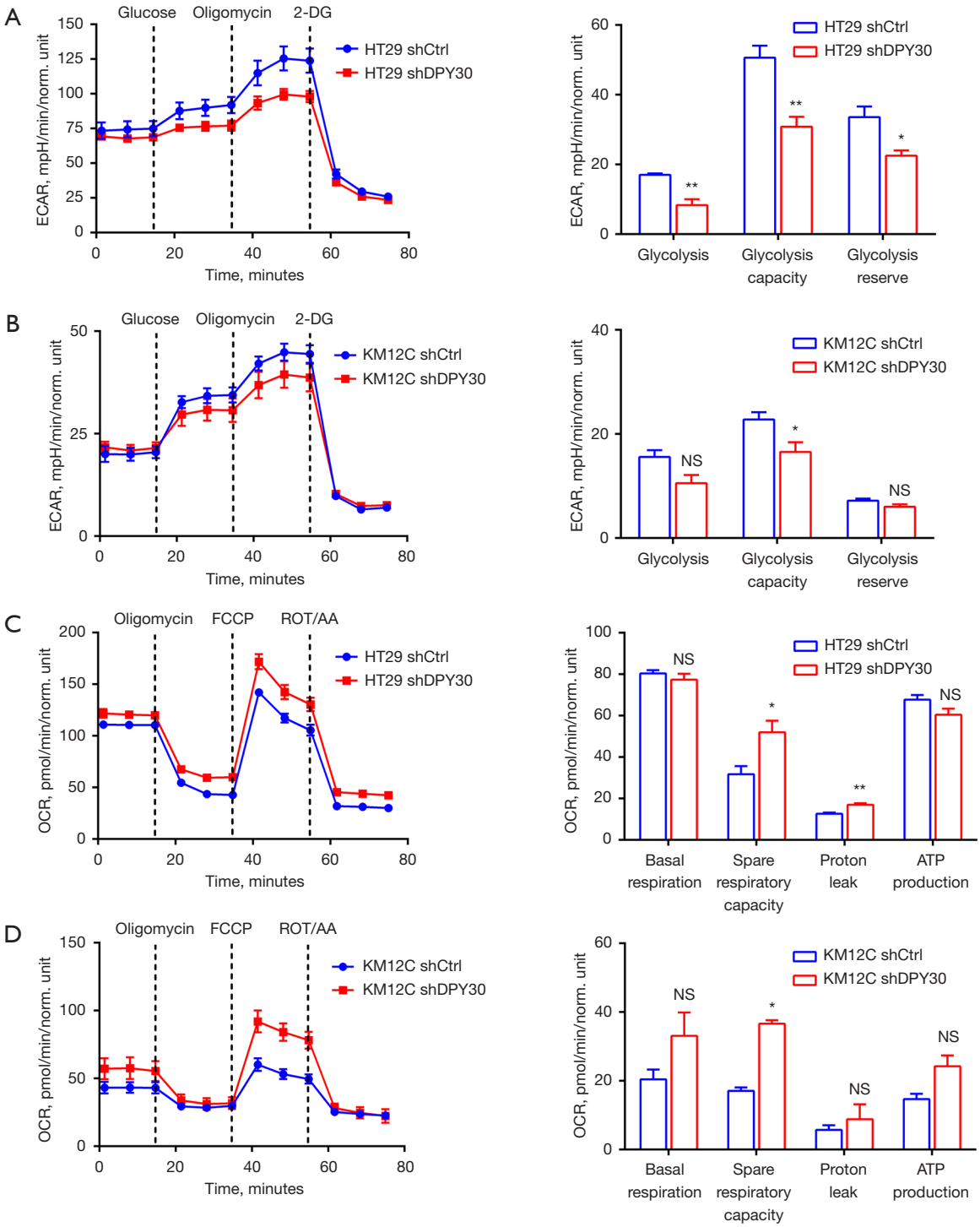

Figure 3 DPY30 knockdown suppressed glycolysis. (A,B) Left, glycolysis flux was examined by measuring the ECAR. Right, the values were calculated by the Seahorse XFe96 software. (C,D) Left, key parameters of mitochondrial function by directly measuring the OCR of cells. Right, the values were calculated by the Seahorse XFe96 software. Data were expressed as mean ± SEM. n=3. *, P<0.05; **, P<0.01. ECAR, extracellular acidification rate; norm., normal; 2-DG, 2-deoxy-d-glucose; sh, short hairpin; NS, no significant difference; OCR, oxygen consumption rate; FCCP, carbonyl cyanide 4-(trifluoromethoxy) phenylhydrazone; ROT, rotenone; AA, antimycin A; ATP, adenosine 5'-triphosphate; SEM, standard error of mean.

(*Figure 4A*). That was to say, H3K4me3 was bound to the promoters of all of these genes, and its binding was significantly decreased after DPY30 knockdown. These results exhibited that DPY30 knockdown inhibited these genes' expression via suppressing the establishment of activated epigenetic modification H3K4me3. However, following the knockdown of DPY30, there was no significant change in the binding of the *GSK3B* promoter. The knockdown of DPY30 exhibited an appreciably inhibitory effect on HT29 xenograft tumor growth (*Figure 4B*), with a significant decrease of tumor weight (*Figure 4C*). In animal models with DPY30 deficiency, HK1 protein expression levels were also reduced (*Figure 4D*). The schematic diagram of this study is shown in *Figure 5*, illustrating that DPY30 promoted the glycolysis of CRC cells through two channels: influencing signaling pathways and gene transcription, thereby promoting the progression of CRC.

Discussion

There is an accumulation of evidence suggesting that many oncogenes and tumor suppressors influence metabolic mode of tumors (23). This study revealed that DPY30 knockdown suppressed aerobic glycolysis of CRC cells via changing the expression of *HK1*, *PFKL*, and *ALDOA*. Those genes are all vital regulators in the process of metabolism (24-26). The previous research has indicated that DPY30 could regulate the expression of *MYC* through H3K4me3. First, DPY30 directly promotes the expression of the *MYC* gene. Second, DPY30 regulates chromatin accessibility and facilitates effective binding of the *MYC* to many genomic targets (27,28). In addition to mediating gene transcription through H3K4me3, DPY30 also regulates various biological activities of CRC cells through signaling pathways. Our results suggested that, following DPY30 knockdown, there was no significant change in the binding of the *GSK3B* promoter to H3K4me3. However, a decrease in the activity of the AKT signaling pathway was detected. The regulation of GSK-3β by the AKT signaling pathway could also be considered in this context.

To date, hundreds of CRC cell lines have been established. KM12C and HT29 cell lines are both established from primary human colon adenocarcinoma. HT29 was initiated from a moderately well-differentiated adenocarcinoma of the colon from a 44-year-old, white, female in 1964 (29,30). The colon carcinoma is classified as tumor-node-metastasis (TNM) stage I. The original KM12 tumor is classified as a poorly differentiated adenocarcinoma, Dukes' stage B_2 (31). As the previous report noted, single cell suspensions obtained from a surgical specimen of primary CRC were directly adapted to growth in culture and designated as line KM12C (32). Because the two cell lines originate from tumors of different grades and stages, they show slightly different results in the experiment. HT29 cells were mainly selected for ChIP assays and the construction of animal model in this study.

Glycolysis is a cascade process catalyzed by a series of enzymes, the first key enzyme of which is hexokinases (HKs). HK catalyzes intracellular glucose phosphorylation to produce glucose 6-phosphate (G-6-P) and consumes one molecule of adenosine 5'-triphosphate (ATP). In humans, four main isoforms of HK have been identified, encoded by the genes *HK1*, *HK2*, *HK3*, and *HK4* (33). *HK1* is widely expressed in almost all mammalian tissues, while *HK2* is typically expressed in insulin-sensitive tissues such as adipose tissue, skeletal muscle, and the heart. *HK3* is often expressed at low levels, while *HK4* is limited to the pancreas and liver. Recent research has revealed that *HK2* is highly expressed in some cancer cells and is associated with poor overall survival rates in cancer patients. HK1 has also been found to participate in the process of some tumors (34-39). For example, the proto-oncogene c-Src enhances the affinity of HK1 to glucose by phosphorylation of HK1, thus promoting the glycolysis of breast cancer cells and accelerating the proliferation and metastasis of breast cancer cells (40). In tumors with KRAS4A mutation, KRAS4A can bind to HK1 on the mitochondrial outer membrane and change the enzyme kinetic characteristics of HK1, so that HK1 is no longer inhibited by G-6-P feedback, and ultimately improve the utilization of glucose by the tumor and accelerate the tumor process (41).

GSK3 consists of two isoforms, GSK-3α and GSK-3β, which are highly homologous. Aberrant activity of the latter has been confirmed to be involved in the occurrence and progression of various diseases. However, strategies targeting GSK-3β for cancer therapy are highly controversial (42). Supporters have commonly observed overexpression and activation of GSK-3β in clinical tumor samples, and both chemical inhibitors of GSK-3β and RNA interference-mediated expression silencing have led to significant tumor growth inhibition (43). However, there are other views that the use of inhibition of GSK-3β as a tumor therapy should be carefully considered. The reason is that β-catenin acts as a classical phosphorylated substrate of GSK-3β, making GSK-3β function as a "tumor

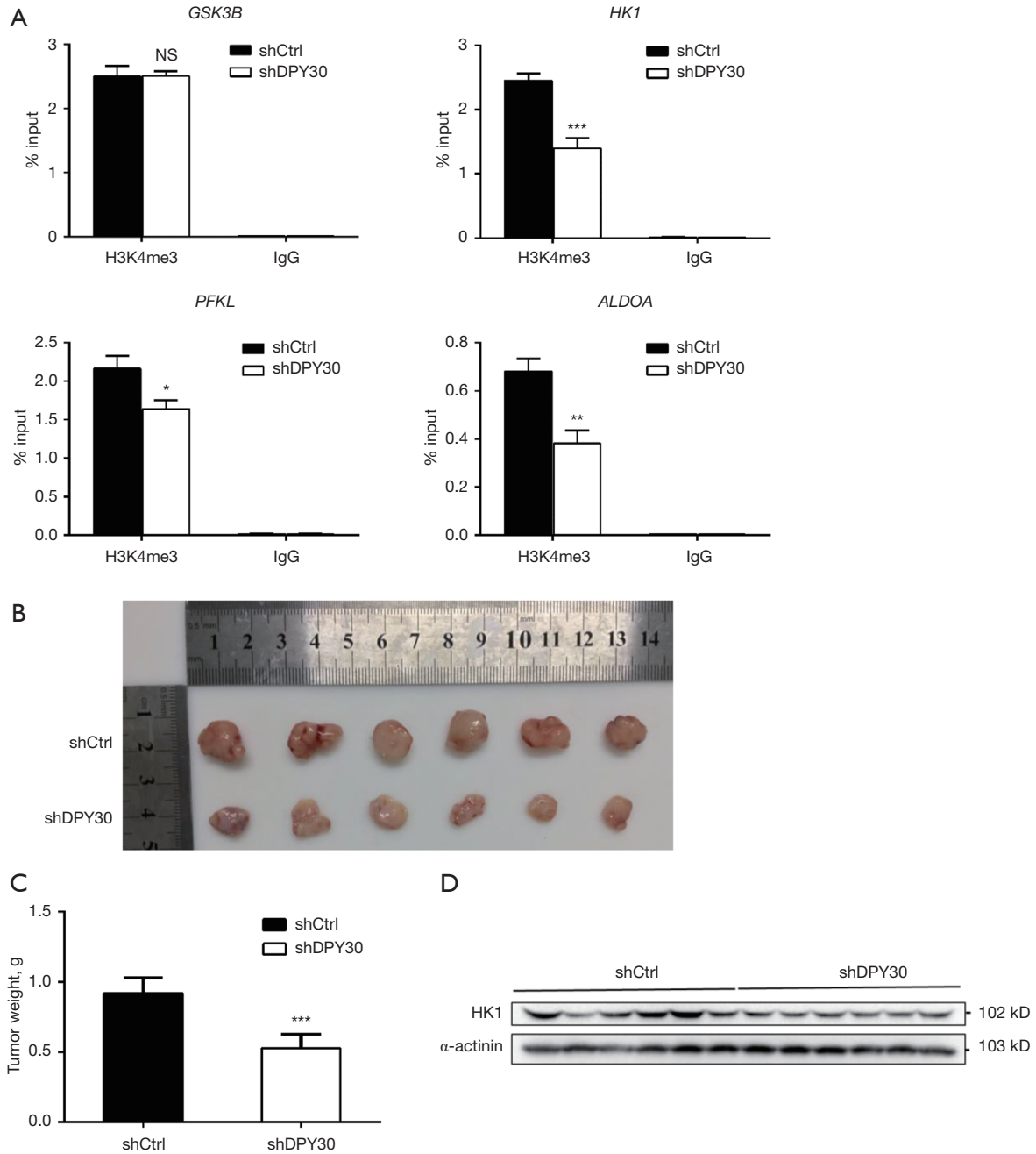

Figure 4 DPY30 knockdown suppressed the establishment of H3K4me3 to target genes. (A) The qPCR assays were performed to evaluate the ChIP analysis of IgG and H3K4me3 interaction status with candidate DPY30 target genes after knockdown assay. H3K4me3 bindings were monitored at the promoters of *GSK3B*, *HK1*, *PFKL*, and *ALDOA*. IgG antibody was included as a negative control. H3K4me3 was normalized to total H3. Values were presented as percentage of input. (B) Images of xenograft tumor in nude mice (n=6). (C) Weight of xenograft tumor in nude mice. (D) The expression levels of HK1 in xenograft tumor were detected by WB. Data were expressed as mean ± SEM. n=3. *, P<0.05; **, P<0.01; ***, P<0.001. IgG, immunoglobulin G; sh, short hairpin; NS, no significant difference; qPCR, quantitative real-time polymerase chain reaction; ChIP, chromatin immunoprecipitation; WB, western blot; SEM, standard error of mean.

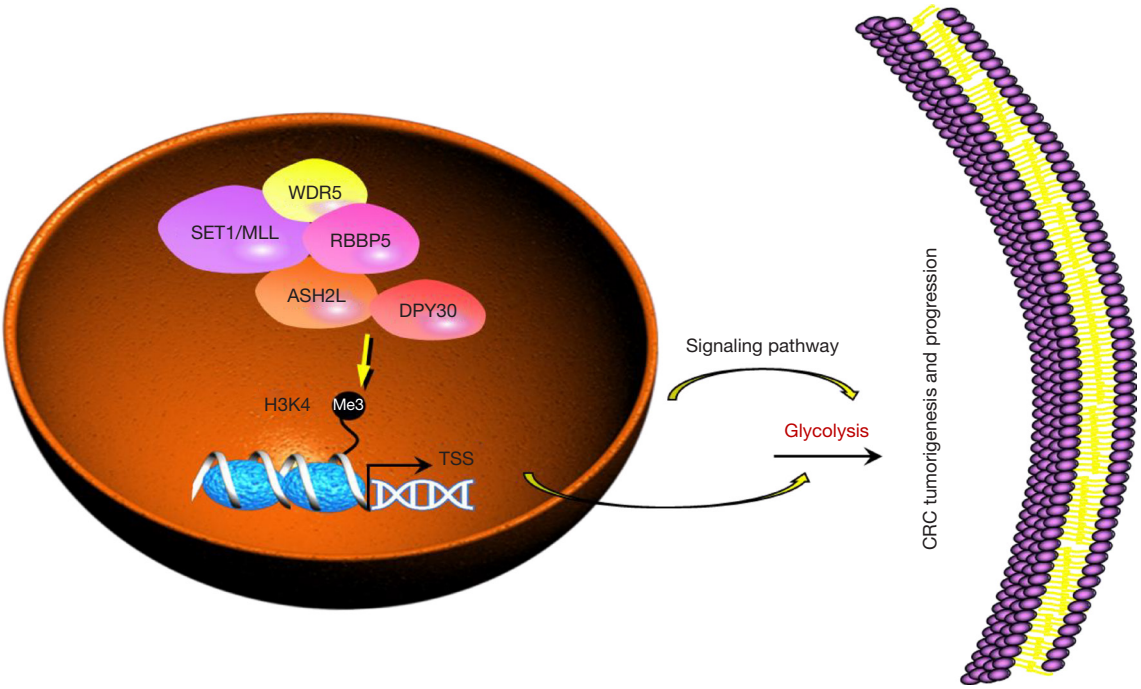

Figure 5 The schematic diagram of this study was created using the elements in the pathway builder. DPY30 promoted the glycolysis of CRC cells through two channels: influencing signaling pathways and gene transcription, thereby promoting the progression of CRC. TSS, transcription start site; CRC, colorectal cancer.

suppressor" in the Wnt signaling pathway. On the one hand, cytoplasmic GSK-3β acts as a switch molecule in the β-catenin degradation complex, leading to its destabilization through phosphorylation of β-catenin and ubiquitin ligase β-TrCP-mediated ubiquitin-proteasome pathway (44). On the other hand, GSK-3β is distributed in the nucleus (45). However, unlike the intracellular mechanism, β-catenin activity is inhibited by a non-phosphorylated pathway. Therefore, the inactivation of GSK-3β activates the Wnt signaling pathway inside and outside the nucleus, thus promoting the progression of tumors (46). Conversely, upregulation of GSK-3β activity can inhibit Wnt signaling and thus reduce the tumor occurrence. Based on this theory, certain compounds have been shown to exert anti-tumor effects by activating GSK-3β and promoting β-catenin degradation (47).

The metabolic regulation of Akt on glucose glycolytic flux may involve multiple mechanisms (48-50). First, Akt can promote glucose uptake by increasing the expression of Glut1, 2, 4, and by regulating the translocation of Gluts to the cell membrane. Second, increased oxidative phosphorylation and glycolysis may kinetically favor the increase of glycolytic flux. Third, highly activated Akt can activate downstream mTORC1, thereby promoting the accumulation of HIF-1a in normoxic conditions (not degraded by VHL), leading to an increase in the enrichment of Glut1, mitochondrial HK, and lactate dehydrogenase (LDH). The increase in glucose transport and uptake, coupled with increased oxidative phosphorylation, results in an increase in the supply and utilization of G-6-P in glycolysis and the pentose phosphate pathway (PPP). Akt inhibits glycogen synthesis and accumulation by inactivating GSK-3β phosphorylation.

Conclusions

This research explored the effects of DPY30 on glycolysis-related genes and proteins from the perspectives of epigenetic changes and signaling pathways, elucidating the role of DPY30 in the glucose metabolism of CRC cells.

Acknowledgments

Funding: This work was supported by the Natural Science Research of Jiangsu Higher Educations of China (Nos. 23KJD180007 and 23KJB350008), the Basic Research

Projects of Taicang (Nos. TC2021JC15, TC2021JC11, TC2022JC27, and TC2022JC32), and the Jiangsu University 'Qing Lan Project' Outstanding Young Key Teachers Subsidy (No. Su Teacher Letter [2023] No. 27).

Footnote

Reporting Checklist: The authors have completed the ARRIVE and MDAR reporting checklists. Available at https://tcr.amegroups.com/article/view/10.21037/tcr-24-366/rc

Data Sharing Statement: Available at https://tcr.amegroups.com/article/view/10.21037/tcr-24-366/dss

Peer Review File: Available at https://tcr.amegroups.com/article/view/10.21037/tcr-24-366/prf

Conflicts of Interest: All authors have completed the ICMJE uniform disclosure form (available at https://tcr.amegroups.com/article/view/10.21037/tcr-24-366/coif). The authors have no conflicts of interest to declare.

Ethical Statement: The authors are accountable for all aspects of the work in ensuring that questions related to the accuracy or integrity of any part of the work are appropriately investigated and resolved. Animal experiments were performed according to ethical guidelines of animal experiment and reviewed and approved by the Institutional Animal Care and Use Ethics Committee of Xiamen University (No. XMULAC20180077), in compliance with national guidelines for the care and use of animals.

References

1. Sung H, Ferlay J, Siegel RL, et al. Global Cancer Statistics 2020: GLOBOCAN Estimates of Incidence and Mortality Worldwide for 36 Cancers in 185 Countries. CA Cancer J Clin 2021;71:209-49.
2. Arnold M, Sierra MS, Laversanne M, et al. Global patterns and trends in colorectal cancer incidence and mortality. Gut 2017;66:683-91.
3. Shao B, Zhu M, Shen K, et al. Disease Burden of Total and Early-Onset Colorectal Cancer in China from 1990 to 2019 and Predictions of Cancer Incidence and Mortality. Clin Epidemiol 2023;15:151-63.
4. Wang Y, Xia Y, Lu Z. Metabolic features of cancer cells. Cancer Commun (Lond) 2018;38:65.
5. Kouzarides T. Chromatin modifications and their function. Cell 2007;128:693-705.
6. Rao RC, Dou Y. Hijacked in cancer: the KMT2 (MLL) family of methyltransferases. Nat Rev Cancer 2015;15:334-46.
7. Vedadi M, Blazer L, Eram MS, et al. Targeting human SET1/MLL family of proteins. Protein Sci 2017;26:662-76.
8. Ali A, Tyagi S. Diverse roles of WDR5-RbBP5-ASH2L-DPY30 (WRAD) complex in the functions of the SET1 histone methyltransferase family. J Biosci 2017;42:155-9.
9. Ruthenburg AJ, Allis CD, Wysocka J. Methylation of lysine 4 on histone H3: intricacy of writing and reading a single epigenetic mark. Mol Cell 2007;25:15-30.
10. Rickels R, Shilatifard A. Enhancer Logic and Mechanics in Development and Disease. Trends Cell Biol 2018;28:608-30.
11. Shilatifard A. The COMPASS family of histone H3K4 methylases: mechanisms of regulation in development and disease pathogenesis. Annu Rev Biochem 2012;81:65-95.
12. Ernst P, Vakoc CR. WRAD: enabler of the SET1-family of H3K4 methyltransferases. Brief Funct Genomics 2012;11:217-26.
13. Zhang H, Li M, Gao Y, et al. Structural implications of Dpy30 oligomerization for MLL/SET1 COMPASS H3K4 trimethylation. Protein Cell 2015;6:147-51.
14. Hsu DR, Meyer BJ. The dpy-30 gene encodes an essential component of the Caenorhabditis elegans dosage compensation machinery. Genetics 1994;137:999-1018.
15. Jiang H, Shukla A, Wang X, et al. Role for Dpy-30 in ES cell-fate specification by regulation of H3K4 methylation within bivalent domains. Cell 2011;144:513-25.
16. He FX, Zhang LL, Jin PF, et al. DPY30 regulates cervical squamous cell carcinoma by mediating epithelial-mesenchymal transition (EMT). Onco Targets Ther 2019;12:7139-47.
17. Zhang L, Zhang S, Li A, et al. DPY30 is required for the enhanced proliferation, motility and epithelial-mesenchymal transition of epithelial ovarian cancer cells.

Int J Mol Med 2018;42:3065-72.
18. Hong ZF, Zhang WQ, Wang SJ, et al. Upregulation of DPY30 promotes cell proliferation and predicts a poor prognosis in cholangiocarcinoma. Biomed Pharmacother 2020;123:109766.
19. Lee YJ, Han ME, Baek SJ, et al. Roles of DPY30 in the Proliferation and Motility of Gastric Cancer Cells. PLoS One 2015;10:e0131863.
20. Liu B. DPY30 functions in glucose homeostasis via integrating activated histone epigenetic modifications. Biochem Biophys Res Commun 2018;507:286-90.
21. Su WC, Mao XM, Li SY, et al. DPY30 Promotes Proliferation and Cell Cycle Progression of Colorectal Cancer Cells via Mediating H3K4 Trimethylation. Int J Med Sci 2023;20:901-17.
22. Allis CD, Jenuwein T. The molecular hallmarks of epigenetic control. Nat Rev Genet 2016;17:487-500.
23. Lu J, Tan M, Cai Q. The Warburg effect in tumor progression: mitochondrial oxidative metabolism as an anti-metastasis mechanism. Cancer Lett 2015;356:156-64.
24. Feng Y, Zhang Y, Cai Y, et al. A20 targets PFKL and glycolysis to inhibit the progression of hepatocellular carcinoma. Cell Death Dis 2020;11:89.
25. Moon JS, Hisata S, Park MA, et al. mTORC1-Induced HK1-Dependent Glycolysis Regulates NLRP3 Inflammasome Activation. Cell Rep 2015;12:102-15.
26. Xie H, Tong G, Zhang Y, et al. PGK1 Drives Hepatocellular Carcinoma Metastasis by Enhancing Metabolic Process. Int J Mol Sci 2017;18:1630.
27. Shah KK, Whitaker RH, Busby T, et al. Specific inhibition of DPY30 activity by ASH2L-derived peptides suppresses blood cancer cell growth. Exp Cell Res 2019;382:111485.
28. Yang Z, Shah K, Busby T, et al. Hijacking a key chromatin modulator creates epigenetic vulnerability for MYC-driven cancer. J Clin Invest 2018;128:3605-18.
29. Chen TR, Drabkowski D, Hay RJ, et al. WiDr is a derivative of another colon adenocarcinoma cell line, HT-29. Cancer Genet Cytogenet 1987;27:125-34.
30. Fogh J, Trempe G. New human tumor cell lines. In: Fogh J. editor. Human tumor cells in vitro. Boston: Springer US, 1975:115-59.
31. Morikawa K, Walker SM, Nakajima M, et al. Influence of organ environment on the growth, selection, and metastasis of human colon carcinoma cells in nude mice. Cancer Res 1988;48:6863-71.
32. Morikawa K, Walker SM, Jessup JM, et al. In vivo selection of highly metastatic cells from surgical specimens of different primary human colon carcinomas implanted into nude mice. Cancer Res 1988;48:1943-8.
33. Heneberg P. Redox Regulation of Hexokinases. Antioxid Redox Signal 2019;30:415-42.
34. Chen QT, Zhang ZY, Huang QL, et al. HK1 from hepatic stellate cell-derived extracellular vesicles promotes progression of hepatocellular carcinoma. Nat Metab 2022;4:1306-21.
35. Hou Y, Zhang Q, Pang W, et al. YTHDC1-mediated augmentation of miR-30d in repressing pancreatic tumorigenesis via attenuation of RUNX1-induced transcriptional activation of Warburg effect. Cell Death Differ 2021;28:3105-24.
36. Liu S, Wang X, Sun X, et al. Oridonin inhibits bladder cancer survival and immune escape by covalently targeting HK1. Phytomedicine 2024;126:155426.
37. Babu VS, Mallipatna A, Dudeja G, et al. Depleted hexokinase1 and lack of AMPKα activation favor OXPHOS-dependent energetics in retinoblastoma tumors. Transl Res 2023;261:41-56.
38. Yang M, Cai W, Lin Z, et al. Intermittent Hypoxia Promotes TAM-Induced Glycolysis in Laryngeal Cancer Cells via Regulation of HK1 Expression through Activation of ZBTB10. Int J Mol Sci 2023;24:14808.
39. Jin J, Guo D, Wang Y, et al. Artesunate Inhibits the Development of Esophageal Cancer by Targeting HK1 to Reduce Glycolysis Levels in Areas With Zinc Deficiency. Front Oncol 2022;12:871483.
40. Zhang J, Wang S, Jiang B, et al. c-Src phosphorylation and activation of hexokinase promotes tumorigenesis and metastasis. Nat Commun 2017;8:13732.
41. Amendola CR, Mahaffey JP, Parker SJ, et al. KRAS4A directly regulates hexokinase 1. Nature 2019;576:482-6.
42. Takahashi-Yanaga F. Activator or inhibitor? GSK-3 as a new drug target. Biochem Pharmacol 2013;86:191-9.
43. Zhou W, Wang L, Gou SM, et al. ShRNA silencing glycogen synthase kinase-3 beta inhibits tumor growth and angiogenesis in pancreatic cancer. Cancer Lett 2012;316:178-86.
44. Jacobs KM, Bhave SR, Ferraro DJ, et al. GSK-3β: A Bifunctional Role in Cell Death Pathways. Int J Cell Biol 2012;2012:930710.
45. Meares GP, Jope RS. Resolution of the nuclear localization mechanism of glycogen synthase kinase-3: functional effects in apoptosis. J Biol Chem 2007;282:16989-7001.
46. Caspi M, Zilberberg A, Eldar-Finkelman H, et al. Nuclear GSK-3beta inhibits the canonical Wnt signalling pathway in a beta-catenin phosphorylation-independent manner. Oncogene 2008;27:3546-55.

47. Tsai KH, Hsien HH, Chen LM, et al. Rhubarb inhibits hepatocellular carcinoma cell metastasis via GSK-3-β activation to enhance protein degradation and attenuate nuclear translocation of β-catenin. Food Chem 2013;138:278-85.
48. Hatzivassiliou G, Andreadis C, Thompson CB. Akt-directed metabolic alterations in cancer. Drug Discov Today 2005;2:255-62.
49. Rowland AF, Fazakerley DJ, James DE. Mapping insulin/GLUT4 circuitry. Traffic 2011;12:672-81.
50. Huang S, Czech MP. The GLUT4 glucose transporter. Cell Metab 2007;5:237-52.

Cite this article as: Mao X, Yang S, Zhang Y, Yang H, Yan D, Zhang L. The role of chromatin modulator DPY30 in glucose metabolism of colorectal cancer cells. Transl Cancer Res 2024;13(8):4205-4218. doi: 10.21037/tcr-24-366

